NPL Report CMMT(A)200

Development of a Pre-pitting Procedure for Turbine Disc Steel

Project DME11:

Stress Corrosion Cracking and
Corrosion Fatigue from Pits

This report represents the deliverable for Task 2, Milestone 3

Shengqi Zhou and Alan Turnbull

July 1999

ISSN 1361-4061

National Physical Laboratory
Teddington, Middlesex, UK, TW11 0LW

Approved on behalf of Managing Director, NPL, by Dr C Lea,

Head, Centre for Materials Measurement and Technology

Development of a Pre-pitting Procedure for Turbine Disc Steel

S Zhou and A Turnbull
Centre for Materials Measurement and Technology
National Physical Laboratory
Teddington
Middlesex
TW11 0LW

Executive Summary

The development of a pre-pitting procedure for a steam turbine disc steel (3% NiCrMoV) was investigated using $Na_2B_4O_7$/NaCl solutions (pH 9.2) of varying relative concentration and with varying applied current. The final procedure established for a typical cylindrical tensile specimen was as follows.

- A solution of 0.02M $Na_2B_4O_7$ +0.01M NaCl is used.
- The specimens are dry ground and cleaned. For cylindrical specimens, the grinding marks are parallel to the length of the specimens.
- A test cell with an Avesta type seal adapted for cylindrical specimens is used to prevent crevice corrosion.
- After the specimen is immersed in the test solution for one hour, a constant anodic current of 10 μA is applied. This leads to initiation and development of a single pit. To minimise corrosion on the periphery of the pit, the solution is gently stirred but the stirring is applied only after the pit has just initiated.

For the test conditions, the variation of the pit depth with time could be expressed by:

$$a = bt^{\beta}$$

where a is the maximum pit depth in μm, t is the time in seconds, and b and β are 5.96 and 0.31 respectively.

Development of a Pre-pitting Procedure for Turbine Disc Steel

Shengqi Zhou and Alan Turnbull
Centre for Materials Measurement & Technology
National Physical Laboratory
Teddington, Middlesex, UK, TW11 0LW

ABSTRACT

A pre-pitting procedure to generate a single pit of "controlled" depth on a steam turbine disc steel has been developed using di-sodium tetraborate/sodium chloride solution. The optimal conditions for controlled pit generation and growth were obtained by varying the ratio of tetraborate to chloride ions and applying an anodic current of 10 μA. The procedure can be used to produce a single pit on a cylindrical specimen, which can be subsequently used for stress corrosion cracking or corrosion fatigue tests. The growth rate and the shape of the pits have been investigated.

INTRODUCTION

Stress corrosion cracking and corrosion fatigue have been dominant causes of failures of steam turbine blades and discs for decades. Pits can facilitate crack development by acting as stress risers, by creating a local solution chemistry conductive to cracking and by removal of passive films. Pit nucleation and development need not occur under 'normal' operating conditions but may be induced during an excursion, such as an outage, a transition in temperature or water chemistry. In a conventional stress corrosion test, the plain test specimen is simply exposed under the appropriate loading conditions and the crack growth rate is determined by measuring the crack depth on the specimen and dividing by the total test time to obtain an average value. The difficulty is that pit growth in service may proceed for years before a crack initiates. In the accelerated laboratory tests, pits may not grow to the critical size for cracking and thus the impact of pitting may be underestimated. Hence, tests to evaluate the evolution of cracks from pits need to be conducted on pre-pitted specimens. In addition, some crack monitoring techniques, such as DC and AC potential drop measurements, require the site of crack initiation to be known for probe attachment. For these reasons, there is a considerable virtue in producing a single or a dominant pit on the test specimen.

In previous work at NPL,[1] a pre-pitting procedure was developed for generating pits with "controlled" depth and of low density on a 12 Cr blade steel. The objective of this study is to establish an electrochemically accelerated procedure for growing a single pit with "controlled" depth for a steam turbine disc steel (3% NiCrMoV).

EXPERIMENTAL

The material tested was a 3% NiCrMoV steel with a low bainitic microstructure, cut from an ex-service turbine disc supplied by PowerGen. The composition of the steel is listed in Table 1.

Table 1 Chemical composition of the 3% NiCrMoV disc steel (mass %)

C	Si	Mn	P	S	Cr	Mo	Ni	V	Cu	Fe
0.30	0.28	0.45	0.017	0.013	0.69	0.27	2.89	0.091	0.21	bal.

Electrochemical and preliminary pitting tests were conducted initially on a disc electrode in order to establish the procedure prior to application to the cylindrical stress corrosion specimens. The working area of the disc electrode was 0.9 cm^2. The cylindrical specimens were manufactured with the longitudinal axis parallel to the radius of the turbine disc, according to ASTM E8.[2] The overall length was 125 mm, the shoulder diameter was16 mm, the gauge length 25.4 mm and the diameter 6.4 mm. The exposed area of the cylindrical specimen was approximately 9.6 cm^2. In the present study, all tests were conducted on the disc specimen, unless stated otherwise.

For both disc and cylindrical specimens, the surface was dry ground to a 2400 SiC grit finish and rinsed in distilled water, ethanol and acetone in an ultrasonic bath before use. For the cylindrical specimens, the final grinding direction, and hence any grinding marks, were parallel to the length of the specimen.

The solutions used are listed in Table 2 and were prepared from AR grade $Na_2B_4O_7$ and NaCl and distilled water. The initial pH of all solutions was 9.2 ± 0.1 and there was no change in the pH during the tests due to the buffering action of $Na_2B_4O_7$. The solution was open to air. The tests were conducted at ambient temperature (21 ± 1 °C).

Table 2 Solutions used and the concentration ratio of $B_4O_7^{2+}$ /Cl^-

Solution	r ($B_4O_7^{2+}$ /Cl^-)
0.05 M $Na_2B_4O_7$ + 0.001 M NaCl	50
0.05 M $Na_2B_4O_7$ + 0.01 M NaCl	5
0.01 M $Na_2B_4O_7$ + 0.005 M NaCl	2
0.002 M $Na_2B_4O_7$ + 0.01 M NaCl	2
0.01 M $Na_2B_4O_7$ + 0.01 M NaCl	1
0.01 M $Na_2B_4O_7$ + 0.05 M NaCl	0.2

For disc specimens, crevice corrosion was prevented using a 0.25 L conventional Avesta cell.[3] For cylindrical specimens, a 0.4 L cell was made with an Avesta seal at both ends of the specimen. In both cells, the base solution with the same concentration of $Na_2B_4O_7$ as the test solution but without NaCl) was pumped at a rate of 2 ml/hour into the region of the seal to limit the build up of an aggressive environment. Solution with twice the concentration of NaCl of the test solution was added continuously to the bulk solution to compensate for the dilution of chloride, albeit small, due to the ingress of the base solution in the seal region.

The electrode potential was measured with respect to an external saturated calomel electrode (SCE) connected through a salt bridge filled with the test solution. A platinum wire was used as the counter electrode. To ensure that the pit formed on the surface of the *gauge* length of the cylindrical specimens the platinum counter electrode was located close to the centre of the specimen.

The depth and the surface width of the pit were measured using a travelling microscope (resolution 1 μm). In the latter case, the maximum width in one direction was measured and the width vertical to this was measured also. The depth and the shape of the pit would be further examined on the fractured surface after stress corrosion testing.

The open circuit potential, polarisation curve and the time dependence of the potential under galvanostatic conditions were measured using a computer controlled potentiostat (ACM Gill 8). The polarisation curves were generated at a scan rate of 1 mV/s after the electrode had been immersed in the solution for 2 hours. The IR drop was not corrected but this should not cause any significant error since the polarisation current was small.

After testing, specimens were cleaned with distilled water, ethanol and acetone in an ultrasonic bath. In pre-pitting of stress corrosion specimens, the chloride in the pit will be removed by applying cathodic polarisation prior to specimen removal and cleaning.

RESULTS AND DISCUSSION

Establishment of the environmental conditions

In order to produce a single pit on the specimen surface in a controlled manner, it is essential to establish an environment in which pitting does not occur at the open circuit potential. On the other hand, the pitting potential in the environment should not be too far from the open circuit potential and well below the oxygen evolution and transpassive potentials. The $Na_2B_4O_7$ solution was chosen as the basis for the test solution, as it is an alkaline buffer solution, facilitating passivation of the disc steel. NaCl was added to induce pitting corrosion. The initial task of the work was to optimise the concentration ratio of $B_4O_7^{2-}/Cl^-$, r, to achieve the right balance of passivity and aggressivity in the environment.

Figs. 1 (a) and (b) show the effect of the concentration ratio of $B_4O_7^{2-}/Cl^-$ on the open circuit potential as a function of time. It can be seen that in solutions with the concentration ratio of $B_4O_7^{2-}/Cl^-$ greater than 2, the electrode is passive (Fig. 1 (a)). The open circuit potential increases with time due to the growth of the passive film. A stable value of the corrosion potential was not achieved in 60 hours. A long term test demonstrated that the open circuit potential took 10 days to reach a relatively stable value of -60 mV (SCE) in 0.05 M $Na_2B_4O_7$ + 0.001 M NaCl solution. It can also be seen that the open circuit potential decreases as the ratio of $B_4O_7^{2-}/Cl^-$ decreases. In 0.01 M $Na_2B_4O_7$ + 0.01 M NaCl and 0.01 M $Na_2B_4O_7$ + 0.05 M NaCl solutions (r of 1 and 0.2 respectively), the passive film is not stable and breaks down under open circuit conditions (Fig. 1 b). The breakdown potential and the time to breakdown decrease as the ratio of $B_4O_7^{2-}/Cl^-$ is decreased. Subsequent examination of the surface revealed that general corrosion had occurred in 0.01 M $Na_2B_4O_7$ + 0.05 M NaCl and localised corrosion in 0.01 M $Na_2B_4O_7$ + 0.01 M NaCl.

The effect of the ratio of $B_4O_7^{2-}/Cl^-$ on the polarisation behaviour of 3% NiCrMoV steel is shown in Figs. 2 (a), (b) and (c). In 0.05 M $Na_2B_4O_7$ + 0.01 M NaCl solution (r = 5), pitting did not occur at potentials below 400 mV (SCE) (Fig. 2 (a)). The anodic current increased with the applied potential, associated with increased metal dissolution and growth of the passive film. The maximum current density in the potential range studied was less than 10 $\mu A/cm^2$ and the anodic current was smaller in the reverse scan than in the forward scan, indicating that no pitting had occurred on the electrode surface. After testing, the surface of the specimen was bright and no pitting was found. Similar behaviour was observed in 0.05 M $Na_2B_4O_7$ + 0.01 M NaCl solution (r = 5). On the other hand, the polarisation curve (Fig. 2 (b)) in 0.01 M $Na_2B_4O_7$ + 0.05 M NaCl solution (r = 0.2) showed that the passive film broke down at a relatively negative potential (-177 mV (SCE)) resulting in a large anodic current. Visual examination of the surface revealed that general corrosion had occurred. In 0.02 M $Na_2B_4O_7$ + 0.01 M NaCl solution, the polarisation curve exhibited behaviour

typical of pitting corrosion (Fig. 2 (c)). The pitting potential (the potential at which the anodic current density reaches 10 μA/cm^2 during the forward scan) was approximately 36 mV (SCE). However, the pitting potential will be dependent on immersion time and potential scan rate.

Clearly, solutions with high concentration ratios of $B_4O_7^{2-}/Cl^-$ ($r \geq 5$) are too passive and solutions with low ratio ($r \leq 1$) are too aggressive to control pit initiation and development. The 0.02 M $Na_2B_4O_7$ + 0.01 M NaCl solution ($r = 2$) provides the balance to meet the requirements of the pre - pitting procedure. The 0.01 M $Na_2B_4O_7$ + 0.005 M NaCl solution ($r = 2$) produced similar results to the 0.02 M $Na_2B_4O_7$ + 0.01 M NaCl solution. However, crevice corrosion often occurred with the former solution due to the relatively low concentration of $Na_2B_4O_7$ in the base solution. Therefore, the pre - pitting procedure was developed in 0.02 M $Na_2B_4O_7$ + 0.01 M NaCl solution.

Development of pre - pitting procedure

The key considerations in establishing a controlled pitting procedure are: potential vs. current control; immersion time; applied current and flow rate. The effect of these factors are described.

- Potential vs. current control

In previous work, a pre-pitting procedure was established for a 12Cr blade steel based on potential control[1]. A potential slightly higher than the pitting potential was applied to initiate pits. The potential was stepped, after pit initiation, to a value below the pitting potential but above the repassivation for the pre-pitted electrode to "shut down" all but the deepest pit. However, it can be seen from Fig. 2 (c) that it is difficult to determine the repassivation potential from the polarisation curve for the 3% NICrMoV steel. Furthermore, the pitting potential depends on the immersion time, as the passive film takes a long time to reach a stable condition. Therefore, a galvanostatic approach was used in the present pre-pitting procedure.

- Immersion time

From Fig. 1 (a), it is clear that the passive film in this system requires a long period to reach a stable condition and this need to be considered when generating the pits. Fig. 3 shows the effect of immersion time at open circuit on the subsequent potential response under galvanostatic polarisation (I = 10 μA). The pitting potential is more noble and the time to pit initiation decreases as the immersion time increases. However, the pit growth rate and the shape of the pits were not significantly affected by the immersion time. Accordingly, a pre-pitting procedure was adopted in which the specimen was immersed in the solution for one hour before application of the anodic current. It is notable that pit growth occurred at a potential of about -200 mV (SCE), comparable to the open circuit potential (Fig. 1 a), suggesting that the accelerated test conditions are not too severe. Microscopic examination of the surface indicated that a single pit had developed.

- Applied current

Pits were also induced by applying an anodic current of 5 μA or 20 μA. With a current of 5 μA, pits were initiated very slowly and there were no visible pits after 1 hour polarisation. On the other hand, multiple pits developed when a current of 20 μA was applied. Therefore, for this system, an anodic current of 10 μA appears to be the optimum choice to ensure that a single pit is generated. Clearly, if the area of the specimen were significantly greater than that herein, the total passive current would change and the applied current would have to reflect this.

- Flow rate

Tests were initially conducted in a static solution. However, examination of the surface revealed that localised corrosion had occurred around the pit due to accumulation of the aggressive solution produced by the pit. Therefore, a series of tests were conducted in stirred solution using a magnetic stirrer. As expected, pitting was very sensitive to the flow rate. When the solution was stirred before the pit initiated, multiple small pits were generated and no pit of any significant depth was produced. Therefore, the solution was stirred only *after* the pit had initiated, i.e. when the potential fell below -200 mV (SCE).

The effect of flow rate on the potential response of the electrode under anodic polarisation at 10 μA is shown in Fig. 4. With a high flow rate, the pit stopped growing after reaching a certain depth, resulting in a sharp increase of the potential and initiation of a new pit. At a lower flow rate, only a single pit formed on the surface with very limited localised attack around the pit mouth. The gradual increase of the potential after about one hour (Fig. 4) reflects the need to supply more driving force for the deeper pit in order to satisfy the fixed current demand.

Since the solution flow in the present study is provided by a magnetic stirrer, the flow rate cannot be defined precisely, although it should be low. The optimum flow rate may depend on the geometry of the specimen and the configuration of the test cell, especially for the cylindrical specimen. However, the stirring speed should be chosen carefully to prevent localised attack around the pit but not to hamper growth of the pit.

Growth rate of pits

The maximum depth of pits generated on both the disc and cylindrical specimens at an applied current of 10 μA is plotted against the time elapsed after pit initiation in Fig. 5. There is no significant difference between the growth rates of the pits generated on the disc and the cylindrical specimens. The rate of increase in potential for the larger cylindrical specimens (9.6 cm^2) was more gradual than for the disc specimens (0.9 cm^2) at constant total current. This can be explained on the basis of the need for a higher potential to supply the current when the specimen area is small. Nevertheless, the gradual thickening of the passive film for the large specimen eventually causes the potential to rise to a value at which the breakdown of the passive film occurs. Once pit initiation had occurred, the potential for both types of specimens dropped to a value similar to that prior to the application of the constant

current. In this circumstance, the applied current is mainly consumed by the growth of the pit; thus, the similar pit growth rate for the different types of specimens.

From linear regression analysis, the pit growth could be described empirically by

$$a = bt^{\beta} \qquad (1)$$

where a is the maximum pit depth in μm, t is the time in seconds, and b and β are 5.96 and 0.31 respectively.

If the applied current is consumed solely by pit growth and the passivation current negligible, the pit depth can be calculated using Faraday's law. For a hemispherical pit this is given by:

$$a = \left(\frac{3MIt}{2zF\pi\rho} \right)^{1/3} \qquad (2)$$

where M if the atomic weight, I is the applied current, t is the time, z is oxidation state of the metal ion, F is Faraday's constant and ρ is the density.

Comparison of the predictions of equation (2) and the experimental data (Fig. 5) suggests that the pit shape is not hemispherical.

Pit geometry

The aspect ratio (the depth of the pits, measured optically, divided by the surface "diameter") is plotted vs. pit depth in Fig. 6. Since the pit mouth is not ideally circular, the aspect ratio of pits was calculated using the average surface "diameter" of pits. The pit geometry is not strictly hemispherical, which would be indicated by an aspect ratio of 0.5. There is a large variation in the data, which may reflect a dependence of pit geometry on the shape of the inclusion from which the pit is initiated. There is no significant difference in the aspect ratio between the pits generated on the disc and cylindrical specimens. The shape of pits on the stress corrosion specimens will be further studied on the fractured surface of the specimens after the stress corrosion tests have been completed.

Application to steam turbine disc stress corrosion tests

The virtue of this technique is that it provides a more effective basis for measuring the growth rate of a crack initiated from a pit.

There is potential concern that the initial development of the crack may be influenced by the method of generating the pit. This cannot be resolved easily but it seems likely that the growth rate of the crack, once initiated, is less likely to be affected. Additionally, the technique of using a constant current means that the pit will tend to develop at the most susceptible microchemistry/microstructure, which will reflect behaviour in service.

When immersed in stress corrosion test solutions, re-activation of the pre-generated pit is not expected to be a problem in aerated solutions.

In deaerated solutions, there is no external electrochemical driving force for pitting. In this case, pitting in service is associated with dissolution of MnS inclusions at the elevated temperature of operation and the effect of the dissolution products on the local electrochemistry. In that context, pitting would be transient. In the pre-generated pit it is likely that existing MnS inclusions would have dissolved out and re-activation would then not be likely. Thus, the presence of such a pit in deaerated solutions would affect only the mechanical driving force for cracking if a crack were to initiate.

CONCLUSIONS

A method of generating individual pits on a steam turbine disc steel has been successfully developed. The procedure involved applying an anodic current of 10 μA to the specimen immersed in a solution of 0.02 M $Na_2B_4O_7$ + 0.01 M NaCl.

REFERENCE

1. S. Zhou and A. Turnbull, “Influence of pitting on the fatigue life of turbine blade steel”, Fatigue & Fracture of Engineering Materials & Structures, to be published.
2. ASTM, E 8 - 94a, Standard Test Methods for Tension Testing of Metallic Materials, (1994).
3. R. Qvarfort, “New electrochemical cell for pitting corrosion testing”, Corrosion Science, **28**, 135-140, (1988).

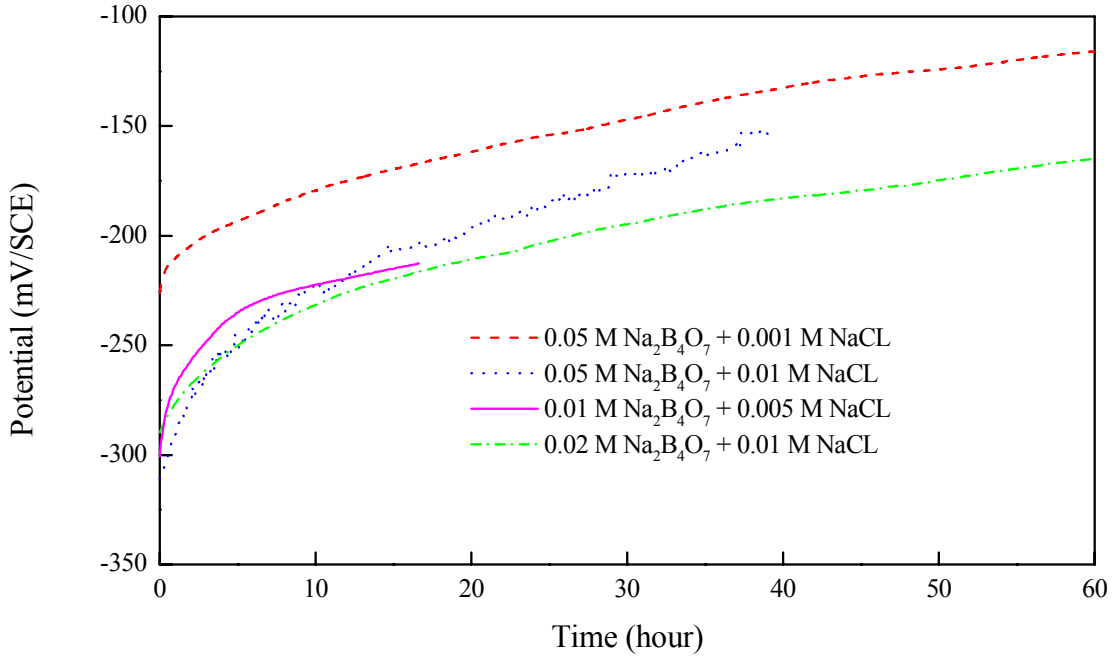

(a)

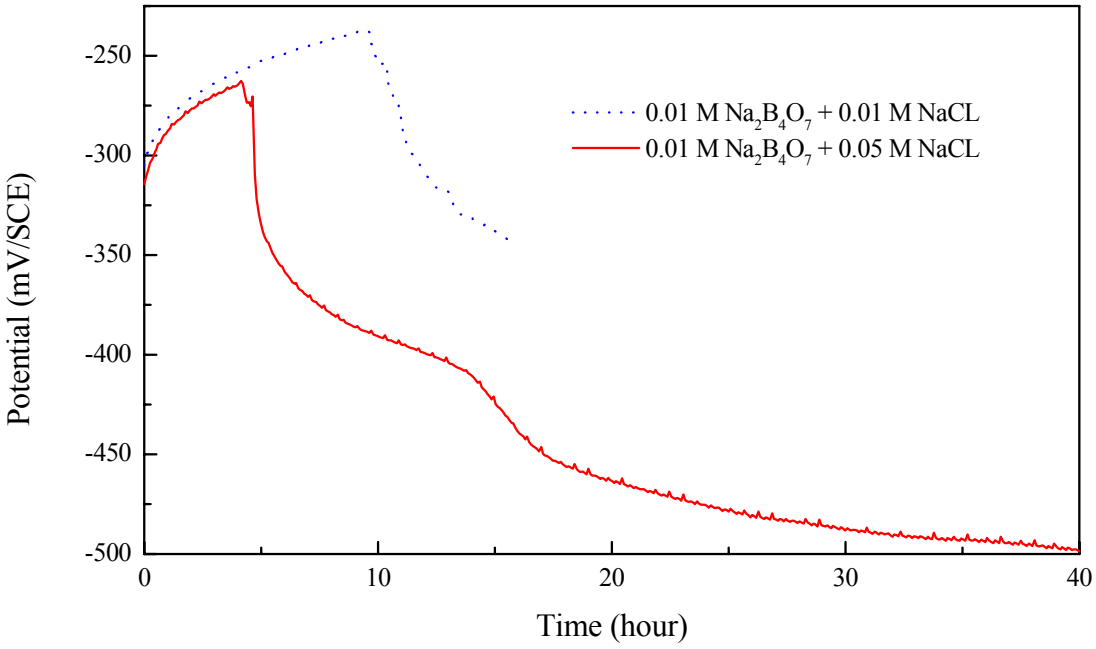

(b)

Fig.1 Effect of the ratio of $B_4O_7^{2-}/Cl^-$ on the open circuit potential of 3% NiCrMoV steel as a function of time.

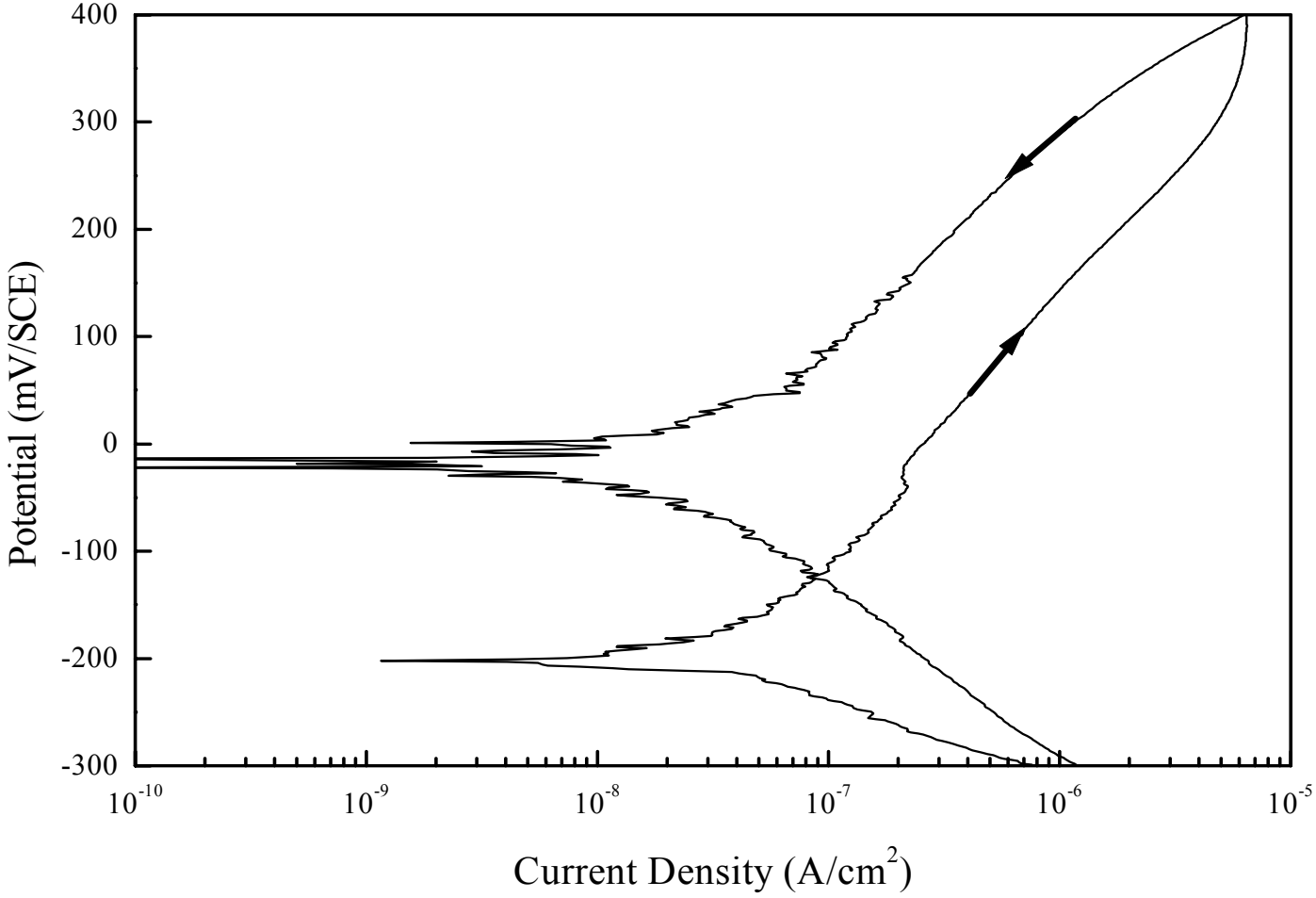

(a) 0.05 M $Na_2B_4O_7$ + 0.01 M NaCl solution

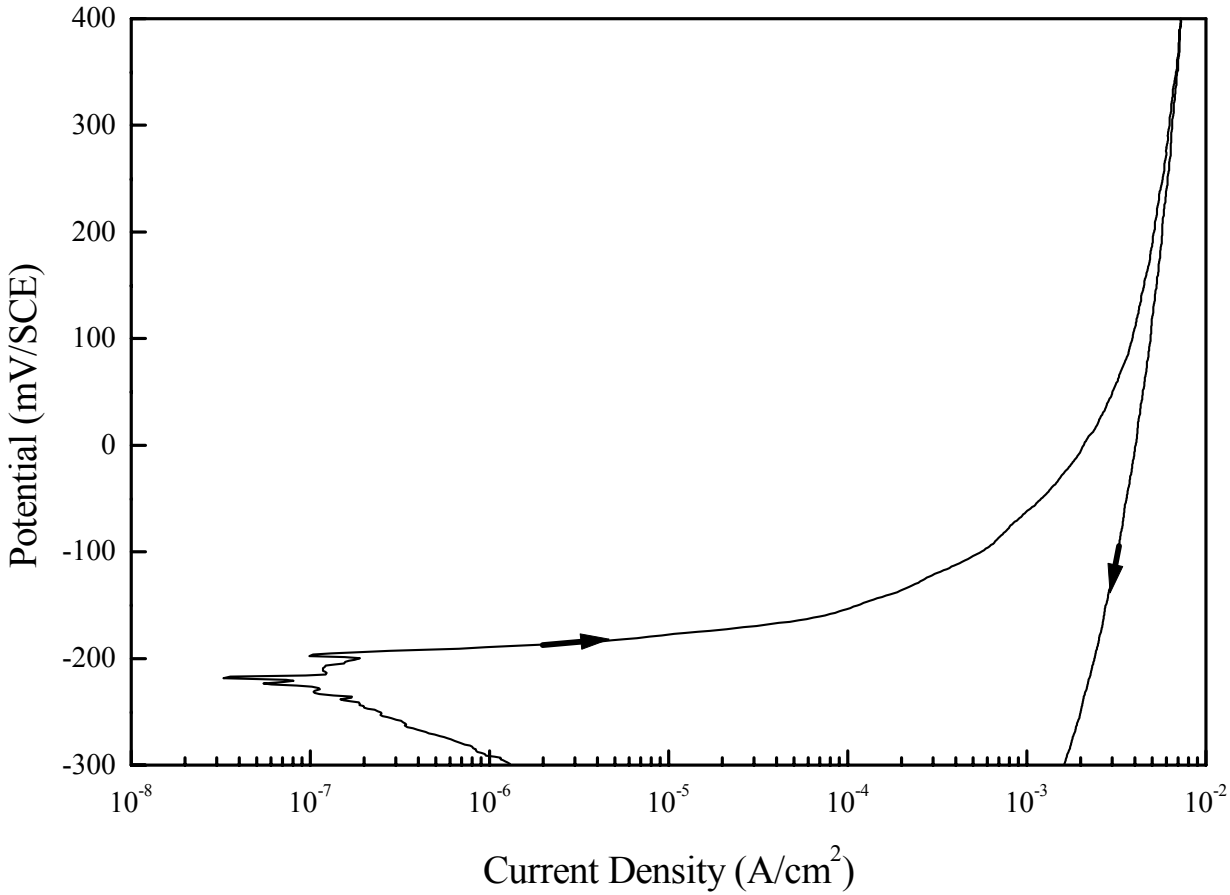

(b) 0.01 M $Na_2B_4O_7$ + 0.05 M NaCl solution

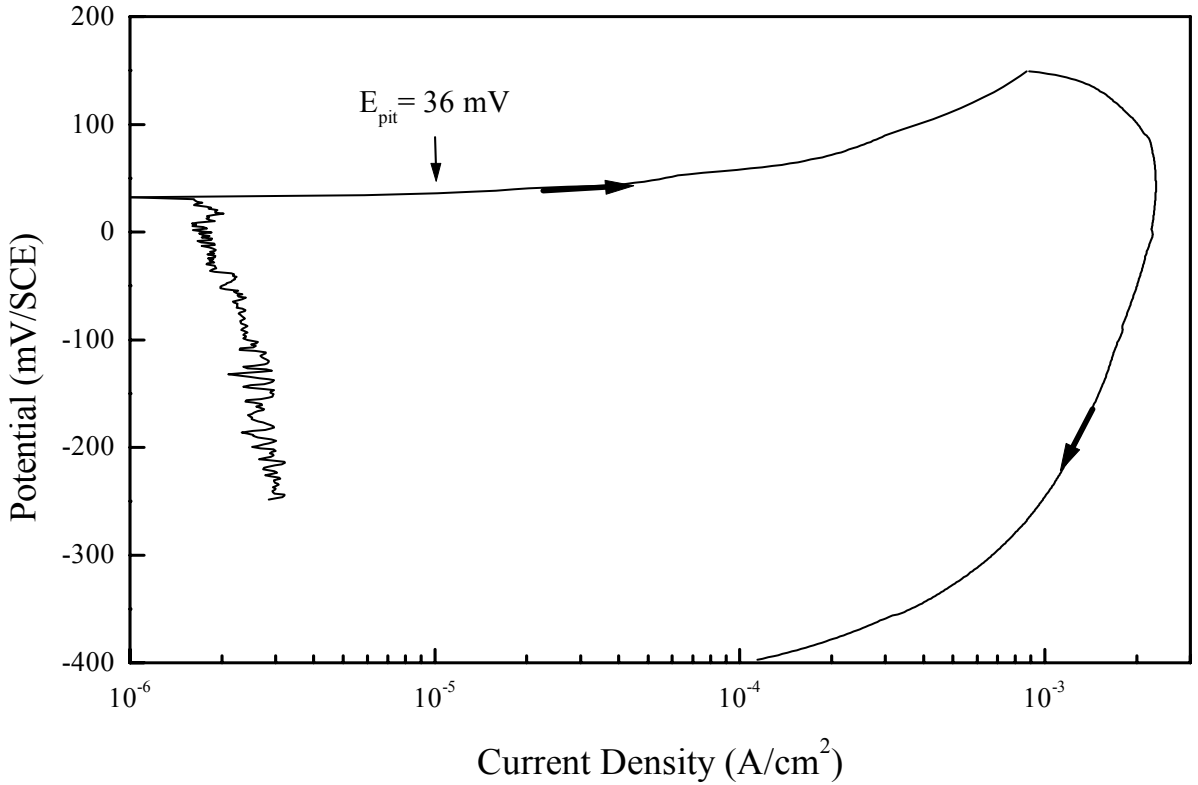

(c) 0.02 M $Na_2B_4O_7$ + 0.01 M NaCl solution

Fig. 2 Effect of the concentration ratio of $B_4O_7^{2-}/Cl^-$ on the polarisation behaviour of 3% NiCrMoV steel

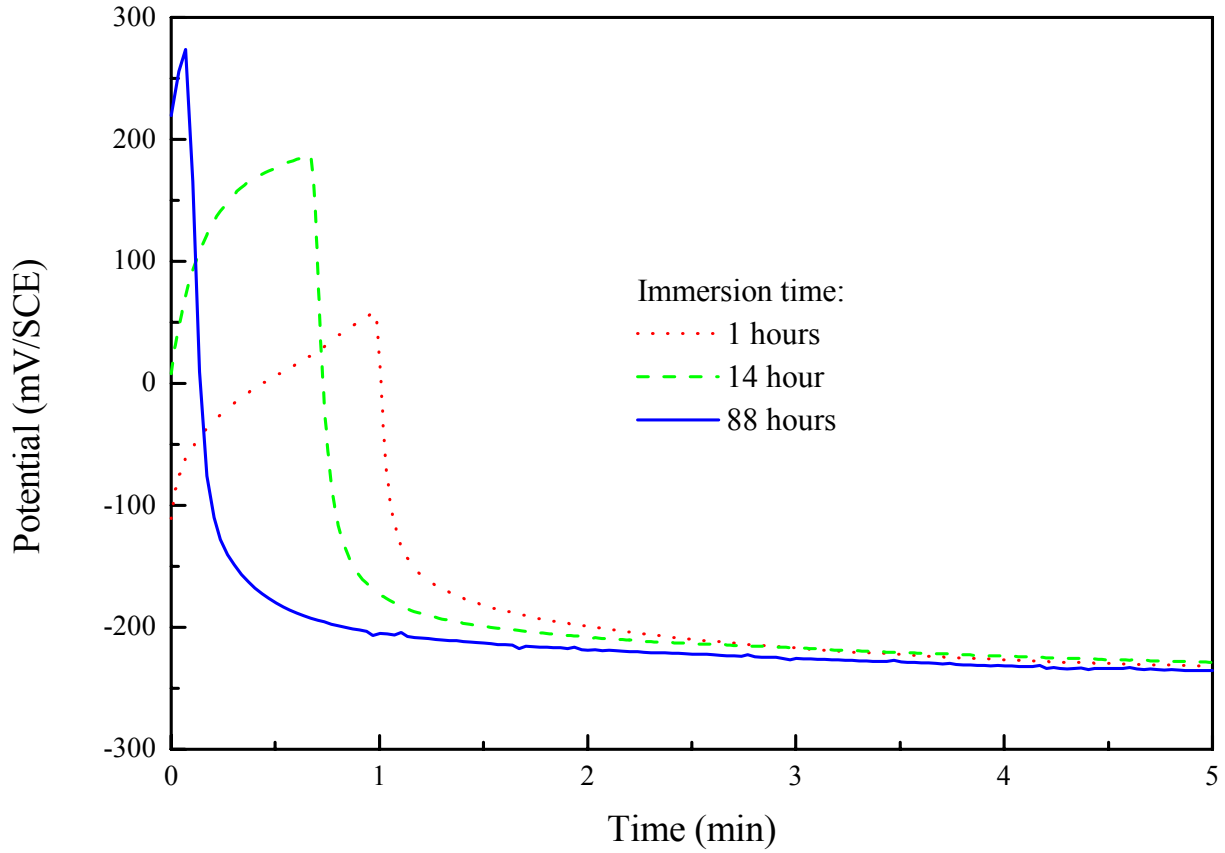

Fig. 3 Effect of immersion time on the pitting potential and the time to pit initiation under galvanostatic polarisation (I = 10 μA).

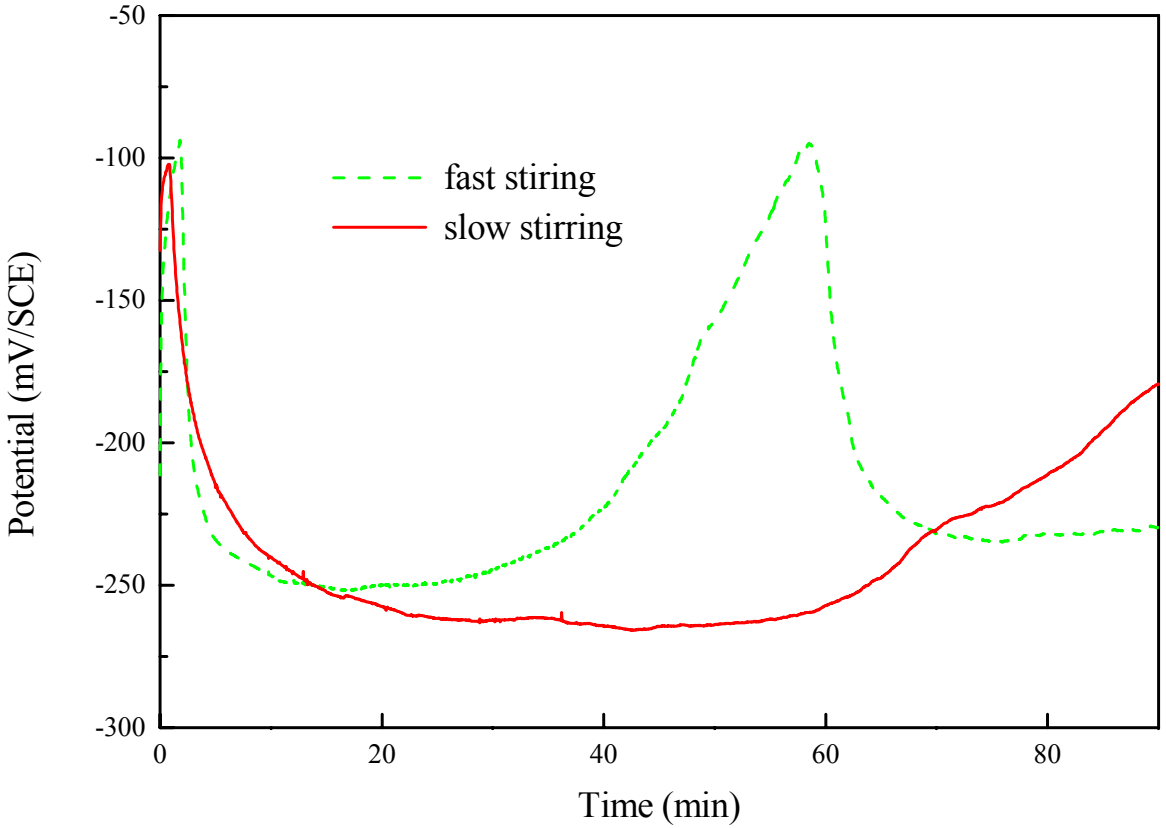

Fig. 4 Effect of the flow rate on the potential response of 3% NiCrMoV steel under galvanostatic polarisation (I = 10 μA).

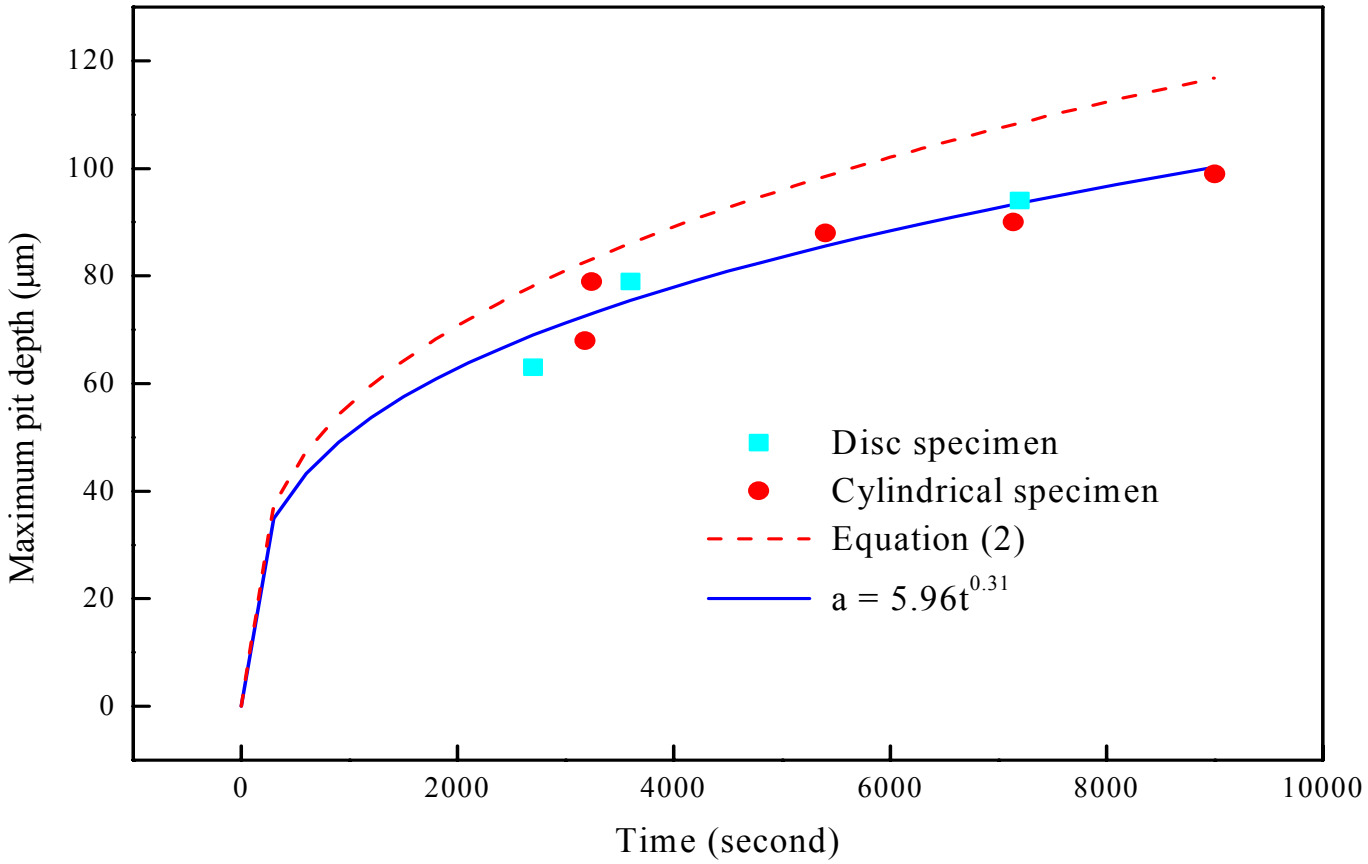

Fig. 5 Time dependence of maximum pit depth of 3% NiCrMnV steel in 0.02M $Na_2B_4O_7$ + 0.01 M NaCl solution

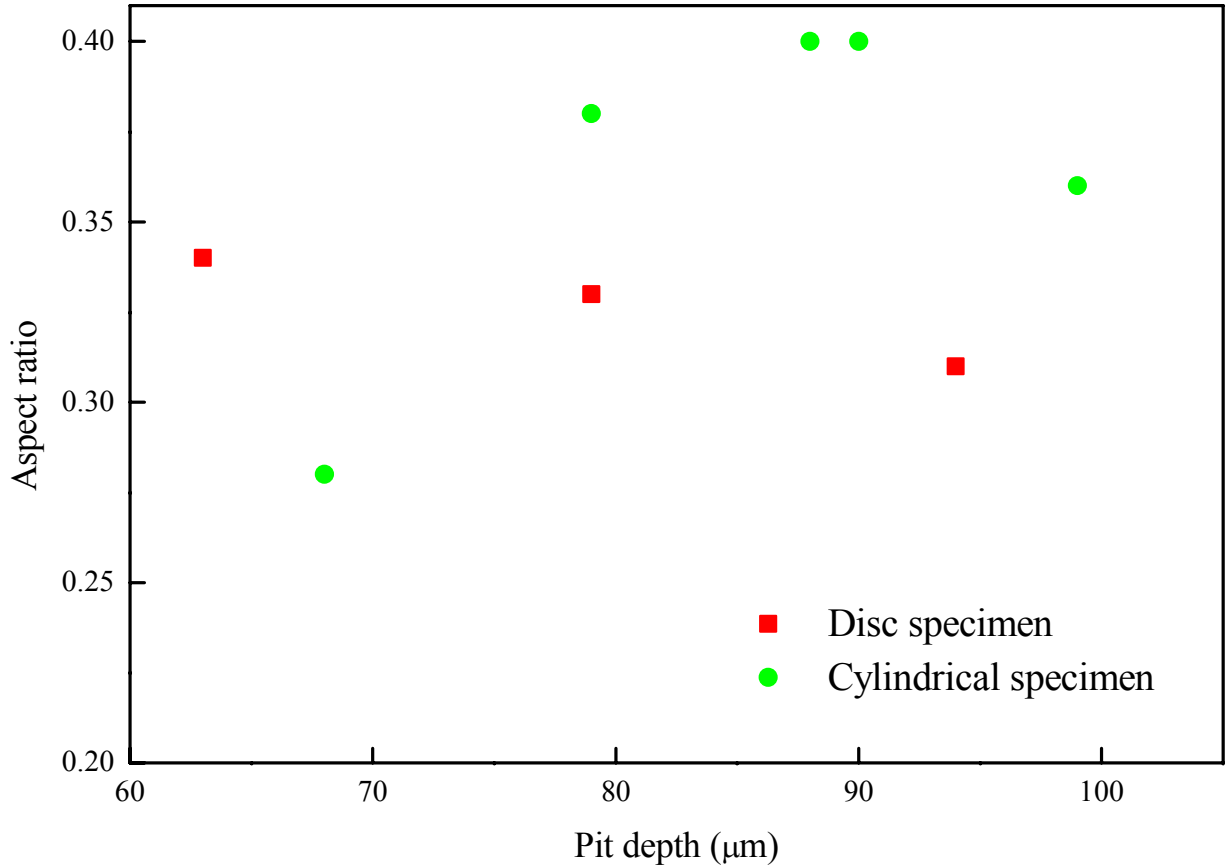

Fig. 6 Aspect ratio of pits as a function of pit depth